

Radiation of an electric charge in the field of a magnetic monopole

Michael Lublinsky^{a,b}, Claudia Ratti^{a,c}, Edward Shuryak^a

^a Department of Physics & Astronomy, State University of New York
Stony Brook NY 11794-3800, USA

^b Physics Department, Ben-Gurion University, Beer Sheva 84105, Israel

^c Department of Theoretical Physics, University of Wuppertal,
Wuppertal 42119, Germany

February 13, 2022

Abstract

We consider the radiation of photons from quarks scattering on color-magnetic monopoles in the Quark-Gluon Plasma. We consider a temperature regime $T \gtrsim 2T_c$, where monopoles can be considered as static, rare objects embedded into matter consisting mostly of the usual “electric” quasiparticles, quarks and gluons. The calculation is performed in the classical, non-relativistic approximation and results are compared to photon emission from Coulomb scattering of quarks, known to provide a significant contribution to the photon emission rates from QGP. The present study is a first step towards understanding whether this scattering process can give a sizeable contribution to dilepton production in heavy-ion collisions. Our results are encouraging: by comparing the magnitudes of the photon emission rate for the two processes, we find a dominance in the case of quark-monopole scattering. Our results display strong sensitivity to finite densities of quarks and monopoles.

1 Introduction

Creating and studying Quark-Gluon Plasma, the deconfined phase of QCD, in the laboratory has been the goal of experiments at CERN SPS and at the Relativistic Heavy Ion Collider (RHIC) facility in Brookhaven National Laboratory, soon to be continued by the ALICE (and, to a smaller extent, by the two other collaborations) at the Large Hadron Collider (LHC). Dileptons and photons are a particularly interesting observable from heavy ion collisions, since electromagnetic probes do not

interact with the medium after their production, thus carrying information about *all* stages of the evolution [1]. Discussion of dilepton production in heavy ion collision experiments at CERN SPS [2, 3] and at RHIC [4] and their comparison to theory can be found in [5, 6, 7], for a recent review see also e.g. [8] and references therein. The main contributions to the production rates considered so far are hadronic decays in the mixed and hadronic phases of the collision (the so-called hadronic cocktail), and quark-antiquark annihilation in the QGP phase. After a long history of experimental studies of dileptons produced by charm decay, NA50/60 experiments finally concluded [9] that they do see QGP radiation, at intermediate dilepton mass range 1-3 GeV, as predicted in [1, 10].

However, the experimentally observed excess in dilepton production at small p_t and small invariant dilepton mass (below $m_\rho \simeq 0.77$ GeV) remains a puzzle: the sum of all known contributions fails to explain the data by a large margin. Motivated by this, we search for additional, unexplored mechanisms which might contribute to the dilepton production rate. In particular, we will focus here on the role played by color-magnetic monopoles: we want to estimate the contribution to dilepton production from quarks which scatter on them. This methodological paper is our initial step towards an exploration of the subject: by no means we claim any resolution of the puzzle.

The so called “magnetic scenario” for QGP [11] suggested that the near- T_c region is dominated by monopoles. More specifically, these authors suggested to look at the magnetic sector as a (magnetic) Coulomb plasma of monopoles in its liquid form. A line of lattice-based results has led to a very similar conclusion [12]. This scenario has met with initial success by providing an explanation of the low viscosity observed at RHIC [11, 13] due to the large transport cross section induced by scattering on monopoles.

Lattice monopoles are defined by the procedure [14] which locates the ends of singular Dirac strings by calculating the total magnetic flux through the boundary of elementary 3-d boxes. Since this depends on a certain gauge fixing, for decades sceptics kept the viewpoint that those objects are just unphysical UV gauge noise. Yet, many specific observables – e.g. monopole density – produced very reasonable and consistent results, apparently independent of the particular lattice parameters [12, 15]. More recent results on monopole correlations [15] quantitatively support the Coulomb plasma picture of Ref. [11], providing further reasons to think that monopoles are not artefacts but meaningful physical objects, present in the QGP as a source of a Coulomb-like magnetic field on which charged particles (quarks) can scatter. We work under the same assumption in the present paper. We are not advocating this magnetic scenario, but rather use it to estimate the contribution of radiation on monopoles. We will not need any assumption about monopole coupling, internal structure or correlations, only their density.

Although we were motivated by the dilepton puzzle and will eventually aim at

solving it as a final goal, we start from the simpler problem of soft photon radiation during the collision process. The emission of real photons is a process which is closely related to dilepton production: the latter takes place through the emission of a virtual photon. In the QGP phase, the leading perturbative diagram is the Compton-like process ($qg \rightarrow q\gamma$ and the crossing diagram $q\bar{q} \rightarrow \gamma g$), while perturbatively subleading bremsstrahlung diagrams ($qq \rightarrow qq\gamma$) and LPM-type resummed effects are in fact equally important [16].

The classical trajectory of a particle with electric charge¹ e in the field of an infinitely heavy monopole with magnetic charge g takes place on the surface of a cone. The static monopole approximation is valid for a regime of temperatures $T \gtrsim 2T_c$, where they can be considered heavy, rare objects embedded into matter consisting mostly of the usual electric quasiparticles, quarks and gluons. The Lorentz force acting on the electric charge is proportional to the product of both couplings (eg). Thanks to the Dirac charge quantization condition, $eg = 1$ and thus it is not a small parameter and it is T -independent.

As a first step towards the solution of the problem, in the present paper we compute the radiation from a non-relativistic electrically charged particle moving in the field of a monopole along the *classical* trajectory, ignoring back reaction. A full quantum and relativistic study is postponed for future investigation. Below we will discuss the applicability limits of our approximation. Therefore, our present calculation cannot address the actual phenomenological questions yet, but we can get an insight into how sizeable the effect of monopoles can be. To this purpose, we will compare our results with the parallel computation of photon emission rate in the process of Coulomb scattering of quarks, in the same approximations, regarding the Coulomb problem as a benchmark for comparison.

Let us start with a “naive estimate” for the ratio of emission rates of quark-monopole vs Coulomb scattering of quarks:

$$\frac{I^{qM}}{I^{qq}} \sim \frac{(eg)^2 v^2}{e^4} \frac{\mu}{m} \frac{n_M}{n_q}. \quad (1)$$

First, the emission amplitude from monopoles is suppressed by the velocity v of the incoming electric particle, because the underlying scattering happens due to Lorentz rather than Coulomb force. Second, it obviously contains the density of monopoles $n_M \sim T^3 / \ln^3(T)$, which is smaller than the quark density $n_q \sim T^3$.

On the other hand, this rate is enhanced by the ratio of coupling constants. The numerator includes the product of the electric gauge coupling constant e and the magnetic one g : in the units we are using, the Dirac quantization condition

¹Here and below we call e the strong interaction coupling constant, using QED-like field normalization of the fields and 4π for consistency with the textbook material we use: note that $e^2 = \alpha_s$. The name g is reserved to color-magnetic coupling, while the electromagnetic coupling will be denoted as e_{em} , again with $e_{em}^2 = \alpha_{em}$.

implies $eg = 1$ (actually \hbar), while the electric Coulomb scattering is proportional to $e^2 = \alpha_s \sim 1/\ln(T) \ll 1$. The $\ln^2(T)$ in the numerator to a significant extent compensates the smallness of the monopole density $n_M \sim 1/\ln^3(T)$. Although formally still decreasing at large T , as is the corresponding ratio of the contributions to viscosity [13], large angle and even backward scattering induced by monopoles may make this ratio numerically enhanced. The reduced mass $\mu = m/2$ enters the Coulomb scattering problem whereas, in the limit of infinite monopole mass, the quark mass m appears in Newton law. There is an additional relative enhancement in favour of monopoles, which is due to the Casimirs of the qq and $q\bar{q}$ potentials. We will work out these factors in the following; they roughly bring a factor $1/4$ compared to the $q - M$ scattering. For typical (thermal) velocity of 0.7 , $\alpha_s = 0.8$, and the ratio of densities 0.2 we end up with a relative effect of order $1/2$. This is obviously a good start, suggesting it is worth to examine the problem in more details.

We will see below that the above crude estimate is indeed correct when the velocity of quarks is sufficiently close to one (we will still be using the non-relativistic approximation); it is also correct in the ultrarelativistic limit. There is, however, a very important effect, which noticeably enhances the relative contribution of monopoles. The above estimate holds for a fixed impact parameter. For soft radiation, only emission from large impact parameters is relevant (and this is the only region where our approximations are in fact valid). However, finite densities of quarks and monopoles in the plasma provide natural cutoffs for maximal impact parameters. Moreover, since the density of monopoles in our temperature regime is much smaller than the density of quarks, the relevant upper cutoff on the impact parameter for the Coulomb problem is much smaller and it leads to a significant suppression of the Coulomb-induced emission rate relatively to the rate due to scattering on monopoles.

Our final results are very encouraging. We find that the soft photon emission rate from quark-monopole scattering could be as large as the mechanisms previously accounted for. Therefore, the problem calls for further and more detailed investigation at the full quantum level, which will be our next step in this project.

The paper is organized as follows. In Section 2 we provide a brief overview of the classical motion of an electric charge in a Coulomb magnetic field: even if these results are well-known, a short summary is useful, since we will make large use of them in the following. In Section 3 we compute the photon radiation rate for an electric particle moving in the field of a static monopole. This section can be regarded as an extra chapter for Ref. [17], in which radiation rates for several trajectories were computed. In Section 4 we present an estimate of our effect in the case of quarks scattering on monopoles in the QGP: we use parameter estimates which are typical of the QGP produced at RHIC. We compare our results with those obtained in the Coulomb problem, and discuss the validity of our approximations. We draw our conclusions in the last Section (5), where we also indicate future

improvements. Appendix A supplements Section 3 by providing details of analytical computations for the emission rate. Appendix B presents a calculation of the quark density in the PNJL model, a result which is needed when we apply our calculations to QGP.

2 Classical quark-monopole scattering

We consider the classical, non-relativistic motion of a charge in an external field [18, 19, 20]. A pointlike magnetic charge g is the source of a Coulomb-like magnetic field

$$\vec{B} = g \frac{\vec{r}}{r^3}. \quad (2)$$

The equation of motion of an electrically charged particle e in such a field is

$$m \frac{d^2 \vec{r}}{dt^2} = e \vec{v} \times \vec{B} = \frac{eg}{r^3} \frac{d\vec{r}}{dt} \times \vec{r}; \quad (3)$$

the static monopole is located at the origin and the vector \vec{r} defines the position of the electric charge (see Fig. 1). In the following, we set $c = 1$ for simplicity. We also use the convention $e^2 = \alpha$, and therefore $eg = 1$.

In this process, the kinetic energy of the electric charge is a constant:

$$E = \frac{mv^2}{2} = \text{const.}, \quad (4)$$

as is the absolute value of the velocity vector v . There is no closed orbit in the charge-monopole system: the electric charge is falling down from infinitely far away

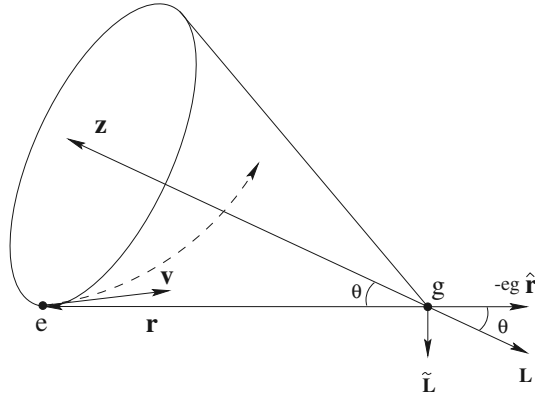


Figure 1: The motion of an electric charge in the field of a magnetic monopole.

onto the monopole, approaching a minimal distance b and being reflected back to infinity. This is evident from the trajectory

$$r = \sqrt{v^2 t^2 + b^2}. \quad (5)$$

A special feature of such a motion is that the conserved angular momentum is different from the ordinary case: the absolute value of the ordinary angular momentum is conserved, but its direction is not constant. The generalized angular momentum

$$\vec{J} = [\vec{r} \times m\vec{v}] - eg \frac{\vec{r}}{r} \quad (6)$$

is an integral of motion. The trajectory of the electric charge does not lie in the plane of scattering orthogonal to the angular momentum; the angle between the vectors \vec{J} and \vec{r} is a constant and the electric charge is moving on the surface of a cone whose axis is directed along $-\vec{J}$ with the cone angle θ defined as:

$$\sin \theta = \frac{mvb}{\sqrt{(mvb)^2 + (eg)^2}}, \quad \cos \theta = \frac{eg}{\sqrt{(mvb)^2 + (eg)^2}}. \quad (7)$$

The velocity of the electrically charged particle is

$$\vec{v} = \frac{d\vec{r}}{dt} = \frac{1}{mr^2} [\vec{J} \times \vec{r}] + \frac{v^2 t}{r} \hat{r} = \frac{1}{mr^2} [\vec{J} \times \vec{r}] + \frac{v}{\sqrt{1 + (b/vt)^2}} \hat{r} = \vec{v}_\varphi \times \vec{r} + v_r \hat{r} \quad (8)$$

where the angular and radial components of the velocity vector are

$$\vec{v}_\varphi = \frac{\vec{J}}{mr^2}, \quad v_r = \frac{v}{\sqrt{1 + (b/vt)^2}}; \quad (9)$$

asymptotically we have

$$v_\varphi \Big|_{t=\pm\infty} = 0, \quad v_r \Big|_{t=\pm\infty} = v, \quad (10)$$

while at the turning point of the path we have

$$v_\varphi \Big|_{t=0} = \frac{\sqrt{(mvb)^2 + (eg)^2}}{mb^2}, \quad v_r \Big|_{t=0} = 0. \quad (11)$$

The azimuthal angle φ as a function of time can be obtained by integrating the angular velocity:

$$\varphi = \frac{1}{\sin \theta} \arctan \frac{vt}{b}. \quad (12)$$

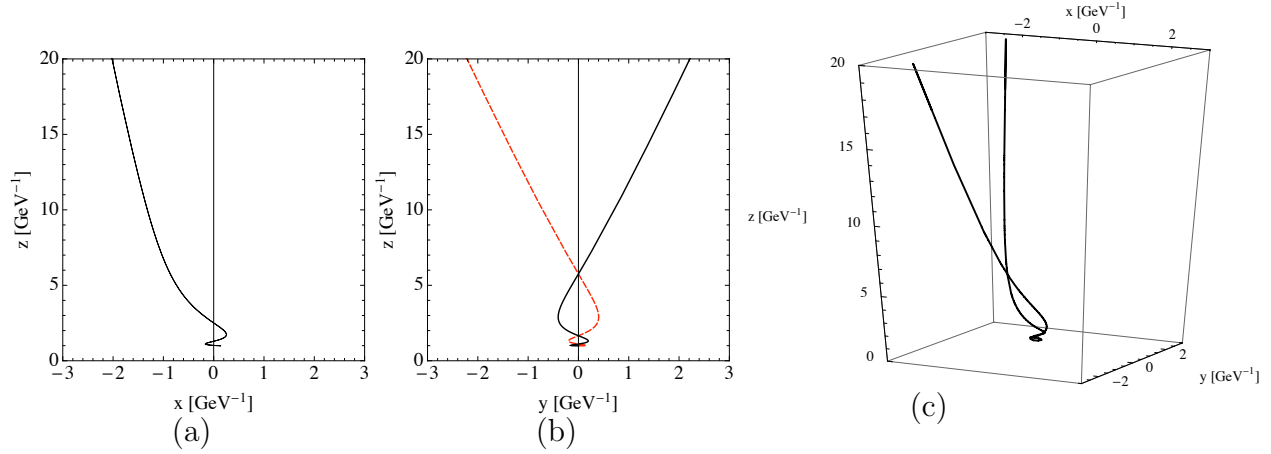


Figure 2: Example of electric charge trajectory in the field of a magnetic monopole. (a) x and z axes: the trajectories of the incoming particle (from $t = -\infty$ to $t = 0$) and the outgoing particle (from $t = 0$ to $t = +\infty$) overlap in this case. (b) y and z axes. Solid line: incoming particle (from $t = -\infty$ to $t = 0$). Dashed: outgoing particle (from $t = 0$ to $t = +\infty$). (c) Three dimensional trajectory. For all plots we use $v = 0.5$; $b = 1 \text{ GeV}^{-1}$, $m = 0.3 \text{ GeV}$.

An example of trajectory is shown in Fig. 2.

The acceleration of the electric charge, $\vec{a} = \frac{d^2\vec{r}}{dt^2}$, follows from Eqs. (3) and (8):

$$\vec{a} = \frac{eg}{mr^3} \vec{v} \times \vec{r} = \frac{eg}{mr^3} (\vec{v}_\varphi \times \vec{r}) \times \vec{r}. \quad (13)$$

We recall that \vec{v}_φ is directed along the z axis (the cone axis) so that:

$$\begin{aligned} \vec{a} &= \frac{eg}{m} \frac{(v_\varphi)_z}{r^3} [r_x r_z, r_y r_z, -(r_x^2 + r_y^2)] \\ &= \frac{eg}{m^2 r^3} \sqrt{(m v b)^2 + (e g)^2} \sin \theta \cos \theta [-\cos \varphi, -\sin \varphi, -\tan \theta]. \end{aligned} \quad (14)$$

3 Radiation

Following Ref. [17] we define the intensity dI of radiation into the element of solid angle $d\Omega$ as the amount of energy passing in unit time through the element $df = R_0^2 d\Omega$ of the spherical surface with center at the origin and radius R_0 . This quantity is equal to the energy flux density ($\vec{S} = \frac{H^2}{4\pi} \vec{n}$) multiplied by df :

$$dI = \frac{H^2}{4\pi} R_0^2 d\Omega. \quad (15)$$

The energy $d\mathcal{E}_{\vec{n}\omega}$, radiated into the element of solid angle $d\Omega$ in the form of waves with frequencies in the interval $d\omega/2\pi$ is obtained from Eq. (15) by replacing the square of the field by the square modulus of its Fourier components and multiplying by 2:

$$d\mathcal{E}_{\vec{n}\omega} = \frac{|\vec{H}_\omega|^2}{2\pi} R_0^2 d\Omega \frac{d\omega}{2\pi} \quad (16)$$

where

$$\vec{H}_\omega = i\vec{k} \times \vec{A}_\omega \quad (17)$$

and

$$\vec{A}_\omega = \frac{e^{ikR_0}}{R_0} \int_{-\infty}^{+\infty} e_{em} \vec{v}(t) e^{i(\omega t - \vec{k} \cdot \vec{r}(t))} dt. \quad (18)$$

We work in the dipole approximation, namely we neglect retardation effects. This approximation is valid provided that $v \ll c$. In this case, the field can be considered as a plane wave, and therefore in determining the field it is sufficient to calculate the vector potential. The intensity of the dipole radiation is:

$$dI = \frac{(e_{em}\vec{a})^2}{4\pi} \sin^2 \theta d\Omega, \quad (19)$$

where \vec{a} is the acceleration of the electric charge. Replacing $d\Omega = 2\pi \sin \theta d\theta$ and integrating over θ from 0 to π , we find the total radiation:

$$I = \frac{2}{3} (e_{em}\vec{a})^2. \quad (20)$$

The quantity $d\mathcal{E}_\omega$ of energy radiated throughout the time of the collision in the form of waves with frequencies in the interval $d\omega/2\pi$ is obtained from Eq. (20) by replacing \vec{a} by its Fourier component \vec{a}_ω and multiplying by 2:

$$d\mathcal{E}_\omega = \frac{4}{3} (e_{em}\vec{a}_\omega)^2 \frac{d\omega}{2\pi}. \quad (21)$$

In a standard planar collision, the total radiation $d\kappa_\omega$ in a given frequency interval $d\omega$ can be obtained by multiplying the radiation $d\mathcal{E}_\omega$ from a single particle (with given impact parameter ρ) by the measure $2\pi\rho d\rho$ and integrating over ρ from ρ_{min} to ρ_{max} . In our case, the motion of the electric particle takes place on the surface of a cone, therefore we have to find the corresponding measure for our process.

If we project the conical motion of the electric particle on a plane orthogonal to \vec{J} , it is possible to define the standard impact parameter ρ for the planar motion [20]. We can define a position vector \vec{R} :

$$\vec{R} = \frac{\hat{J} \times (\vec{r} \times \hat{J})}{\cos \theta} = \frac{1}{\cos \theta} \left[\vec{r} - \hat{J} (\vec{r} \cdot \hat{J}) \right], \quad (22)$$

which is the projection of \vec{r} onto the plane perpendicular to \vec{J} , times a factor $1/\cos\theta$ chosen so that \vec{R} and \vec{r} have the same length. At $t = -\infty$ we have:

$$\dot{\vec{R}}_{-\infty} = \frac{1}{\cos\theta} \left[\vec{v} - \hat{J} (\vec{v} \cdot \hat{J}) \right]. \quad (23)$$

The mechanical angular momentum of the projected motion is the same as the conserved total angular momentum of the motion in the monopole field:

$$\vec{J} = m\vec{R} \times \dot{\vec{R}}; \quad |\vec{J}| = m\rho|\dot{\vec{R}}_{-\infty}|. \quad (24)$$

From the above Equation we get:

$$\rho = \frac{\sqrt{(mb)^2 + (eg)^2}}{mv} \quad (25)$$

from which it is easy to obtain that $\rho d\rho = bdb$: the measure over which we need to integrate $d\mathcal{E}_\omega$ turns out to be equal to bdb for the conical motion. Therefore, we can identify b as the real impact parameter for the process that we are considering (b is actually the minimal distance between the electric particle and the monopole, which is reached at $t = 0$):

$$\frac{d\kappa_\omega}{d\omega} = \int_{b_{min}}^{b_{max}} 2\pi b db \frac{d\mathcal{E}_\omega}{d\omega}. \quad (26)$$

The limits of integration for b are related to the specific scattering process we are dealing with. For example, if we consider a single quark scattering on a single monopole, we have $b_{max} \rightarrow \infty$, while b_{min} can be identified with the size of the monopole core. In the problem we are considering, in which there is a finite density of monopoles, b_{max} turns out to be finite, as we will see in the next Section.

We start by calculating the total radiation throughout the time of the collision following Eq. (20):

$$\mathcal{I} = \int_{-\infty}^{\infty} I(t) dt = \frac{2}{3} \alpha_{em} \int_{-\infty}^{\infty} |\vec{a}(t)|^2 dt; \quad (27)$$

the acceleration components in the coordinate space are given in Eq. (14). We obtain:

$$I(t) = \frac{2}{3} \alpha_{em} \frac{(eg)^2 v^2 b^2}{m^2 r(t)^6} = \frac{2}{3} \alpha_{em} \frac{(eg)^2 v^2 b^2}{m^2 (v^2 t^2 + b^2)^3} \quad (28)$$

so that:

$$\mathcal{I} = \frac{2}{3} \alpha_{em} \frac{(eg)^2 v}{m^2 b^3} \int_{-\infty}^{\infty} \frac{d\tau}{(\tau^2 + 1)^3} = \frac{\pi}{4} \alpha_{em} \frac{(eg)^2 v}{m^2 b^3}; \quad (29)$$

the total radiation can be obtained in the following way:

$$\kappa = \int_{b_{min}}^{b_{max}} 2\pi b db \mathcal{I} = \frac{\pi^2}{2} \alpha_{em} \frac{(eg)^2 v}{m^2} \left(\frac{1}{b_{min}} - \frac{1}{b_{max}} \right). \quad (30)$$

We now proceed by calculating the Fourier transform of the acceleration \vec{a} in the case of quark-monopole scattering:

$$(a_x)_\omega = -\frac{(eg)^2}{m^2 b^2 v \xi} \int_{-\infty}^{\infty} dt \frac{\exp[i\bar{\omega}t] \cos[\xi \arctan t]}{(t^2 + 1)^{3/2}} \quad (31)$$

$$(a_y)_\omega = -\frac{(eg)^2}{m^2 b^2 v \xi} \int_{-\infty}^{\infty} dt \frac{\exp[i\bar{\omega}t] \sin[\xi \arctan t]}{(t^2 + 1)^{3/2}} \quad (32)$$

$$(a_z)_\omega = -\frac{(eg)^2}{mb\xi} \int_{-\infty}^{\infty} dt \frac{\exp[i\bar{\omega}t]}{(t^2 + 1)^{3/2}} \quad (33)$$

where

$$\xi = \frac{\sqrt{(mbv)^2 + (eg)^2}}{mbv}, \quad \bar{\omega} = \omega \frac{b}{v}. \quad (34)$$

For positive ω we obtain (see Appendix A):

$$\begin{aligned} (a_x)_\omega &= \frac{(eg)^2}{m^2 b^2 v \xi} \left\{ \exp(-\bar{\omega}) \cos\left(\frac{\pi\xi}{2}\right) \left[\frac{1}{4} \Gamma\left(\frac{1}{2}(\xi-1)\right) U\left(\frac{1}{2}(\xi-1), -1, 2\bar{\omega}\right) \right. \right. \\ &+ \frac{4p! \Gamma\left(-p + \frac{\xi+3}{2}\right)}{\xi^2 - 1} \sum_{k=0}^p \frac{(-\bar{\omega})^k}{k! (p-k)! \Gamma\left(\frac{\xi-3}{2} - p + k + 1\right)} \times \\ &\left. \left. \times 2^{k-2} \Gamma\left(p - \frac{\xi+1}{2}\right) U\left(p - \frac{\xi+1}{2}, k-1, 2\bar{\omega}\right) \right] \right\} \end{aligned} \quad (35)$$

$$\begin{aligned} (a_y)_\omega &= -\frac{(eg)^2}{m^2 b^2 v \xi} \left\{ i \exp(-\bar{\omega}) \cos\left(\frac{\pi\xi}{2}\right) \left[\frac{1}{4} \Gamma\left(\frac{1}{2}(\xi-1)\right) U\left(\frac{1}{2}(\xi-1), -1, 2\bar{\omega}\right) \right. \right. \\ &- \frac{4p! \Gamma\left(-p + \frac{\xi+3}{2}\right)}{\xi^2 - 1} \sum_{k=0}^p \frac{(-\bar{\omega})^k}{k! (p-k)! \Gamma\left(\frac{\xi-3}{2} - p + k + 1\right)} \times \\ &\left. \left. \times 2^{k-2} \Gamma\left(p - \frac{\xi+1}{2}\right) U\left(p - \frac{\xi+1}{2}, k-1, 2\bar{\omega}\right) \right] \right\} \end{aligned} \quad (36)$$

$$(a_z)_\omega = -\frac{2eg\bar{\omega}}{mb\xi} K_1(\bar{\omega}), \quad (37)$$

where p is the smallest integer number larger than $(\xi + 3)/2$. $p - 2$ is the number of full rotations around z axis. $U(a, b, z)$ is the confluent hypergeometric function with integral representation:

$$U(a, b, z) = \frac{1}{\Gamma(a)} \int_0^\infty e^{-zt} t^{a-1} (1+t)^{b-a-1} dt \quad (38)$$

and $K_n(z)$ is the modified Bessel function of the second kind:

$$K_n(z) = \frac{\Gamma(n + \frac{1}{2})(2z)^n}{\sqrt{\pi}} \int_0^\infty \frac{\cos t \, dt}{(t^2 + z^2)^{n+1/2}}. \quad (39)$$

Equations (35)-(36) are strictly valid for $\omega \geq 0$ and for any value of ξ , except odd, integer numbers. When ξ is an odd integer number, the above formulas vanish identically, and the integral is given by Eq. (65) (see Appendix A). The behavior of $(a_x)_\omega$, $(a_y)_\omega$ and $(a_z)_\omega$ as functions of ω and b is shown in the two panels of Fig. 3. The component $(a_y)_\omega$ is purely imaginary and vanishes at $\omega = 0$. The values of the acceleration components at $\omega = 0$ are:

$$(a_x)_{\omega=0} = \frac{2v}{\xi} \cos \left[\frac{\pi\xi}{2} \right]; \quad (a_y)_{\omega=0} = 0; \quad (a_z)_{\omega=0} = -\frac{(eg)}{mb\xi}. \quad (40)$$

The subleading small ω asymptotic behavior can be found in Appendix A. The photon emission rate is finite as $\omega \rightarrow 0$. It is of course how it should be: the corresponding number of photons $dN_\omega = dI_\omega/\hbar\omega$ would show standard logarithmic IR divergence.

4 Application to QGP

In this Section we give a rough estimate of the effect that we are describing, in the case in which the electric charge is a quark q (or an antiquark \bar{q}), scattering on a color-magnetic monopole in a deconfined medium. The medium contains a finite density of quarks and monopoles. We will compare our result to the radiation produced from Coulomb scattering of $q\bar{q}$, $\bar{q}\bar{q}$ and qq pairs. We consider a regime of temperatures $\gtrsim 2 T_c$ where, according to the magnetic scenario proposed in [11], monopoles can be considered as heavy, static particles.

A quark moving in a deconfined medium acquires a thermal mass due to its interaction with the other particles of the medium. Lattice results for this quantity are available for three values of the temperature [21, 22]. At $T = 1.5T_c$ and $T = 3T_c$ they find $m = 0.8T$, while at $T = 1.25T_c$ they obtain $m = 0.77T$. At $T = 2T_c$ we therefore assume a value of $m \simeq 0.8T$, namely $m \simeq 0.3$ GeV. For temperatures $T \simeq 2T_c$, we can assume that quarks move with an average velocity $v \sim 0.5 - 0.7$.

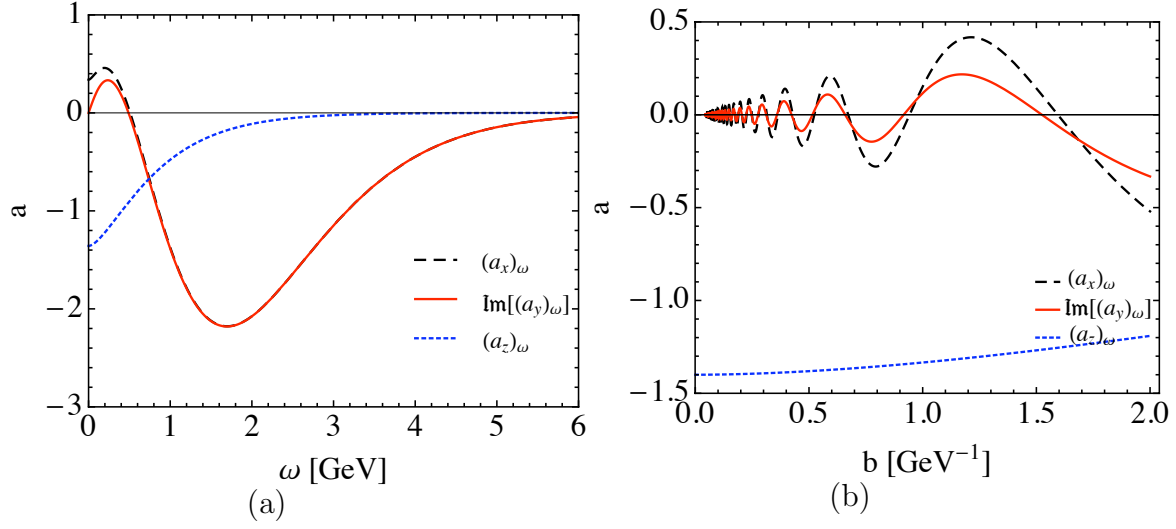


Figure 3: (a): Fourier components of the acceleration as functions of ω , for $m = 0.3$ GeV, $b = 1$ GeV $^{-1}$, $v = 0.7$. (b): Fourier components of the acceleration as functions of b , for $m = 0.3$ GeV, $\omega = 0.1$ GeV, $v = 0.7$.

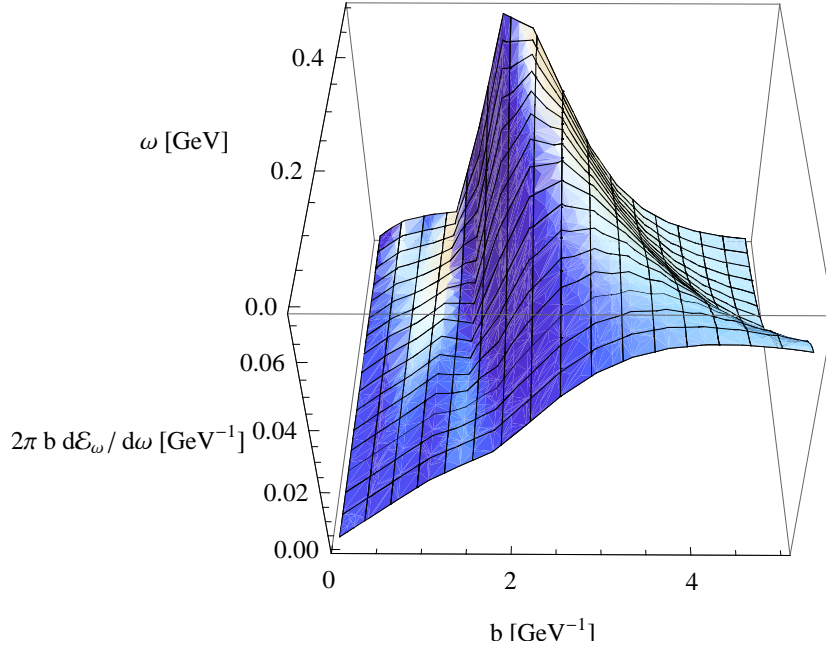


Figure 4: Integrand $2\pi b d\mathcal{E}_\omega/d\omega$ as a function of ω and b . In this figure, $m = 0.3$ GeV and $v = 0.7$.

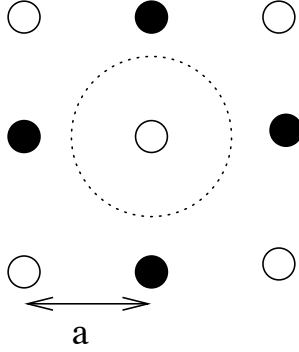


Figure 5: A charge scattering on a 2-dimensional array of correlated monopoles (open points) and antimonopoles (closed points). The dotted circle indicates a region of impact parameters for which scattering on a single monopole is a reasonable approximation.

In Figure 4 we show the integrand for the total radiation in a given frequency interval, namely $2\pi b d\mathcal{E}_\omega/d\omega$, as a function of ω and b . We need to integrate this quantity over the impact parameter. There is no upper limit on b in the case of scattering of one quark on one monopole. However, in matter there is a finite density of monopoles, so the scattering issue should be reconsidered. A sketch of the setting, assuming strong correlation of monopoles into a crystal-like structure, is shown in Fig. 5. A “sphere of influence of one monopole” (the dotted circle) gives the maximal impact parameter to be used

$$b_{max} = n_M^{-1/3}/2. \quad (41)$$

The same is true for the quark-quark and quark-antiquark Coulomb scattering to which we will compare our results. The monopole density as a function of the temperature for $SU(2)$ gauge theory has been evaluated on the lattice [15]. In order to account for the transition from $SU(2)$ to $SU(3)$ gauge group, we scale these results by a factor 2: in $SU(2)$ there is in fact one monopole species while in $SU(3)$ there are two, identified by two different $U(1)$ subgroups. The monopole density at $T \simeq 2T_c$ is $n_M \simeq 0.02 \text{ GeV}^3$, which gives $b_{max} \simeq 1.8 \text{ GeV}^{-1}$. The lattice also gives us information about the monopole size [23]: they turn out to be very small objects, having a radius $r_M \simeq 0.15 \text{ fm} = 0.78 \text{ GeV}^{-1}$. This is the b_{min} that we will use in our integration.

We therefore obtain, for the total energy radiated in unit volume throughout the time of the collision in a given frequency interval:

$$\frac{d\Sigma}{d\omega} = \frac{2}{9} \frac{d\kappa_\omega}{d\omega} n_q n_M = \frac{2}{9} n_q n_M \frac{2}{3\pi} \alpha_{em} 2\pi \int_{b_{min}}^{b_{max}} b |\vec{a}_\omega|^2 db \quad (42)$$

where the factor $\frac{2}{9} = \frac{1}{3}(\frac{4}{9} + \frac{1}{9} + \frac{1}{9})$ comes from the different electric charges for u , d and s quarks (the density of quarks n_q is the sum of the densities of u , d and s quarks).

4.1 Comparison with Coulomb scattering

In this Section we give an estimate of the radiation produced in the scattering of qq , $q\bar{q}$ and $\bar{q}\bar{q}$ pairs in the plasma. In the case of an attractive interaction between particles (namely in the singlet channel for the $q\bar{q}$ scattering and the antitriplet channel for the qq and $\bar{q}\bar{q}$ scatterings), the formula for $d\mathcal{E}_\omega/d\omega$ reads [17]:

$$\frac{d\mathcal{E}_\omega}{d\omega} = \frac{2\pi\alpha^2\omega^2}{3v^4} \left(\frac{(e_{em})_1}{m_1} - \frac{(e_{em})_2}{m_2} \right)^2 \left\{ \left[H_{i\nu}^{(1)'}(i\nu\epsilon) \right]^2 + \frac{\epsilon^2 - 1}{\epsilon^2} \left| H_{i\nu}^{(1)}(i\nu\epsilon) \right|^2 \right\} \quad (43)$$

where:

$$\nu = \frac{\omega\alpha}{\mu v^3}, \quad \epsilon = \sqrt{1 + \frac{\mu^2 b^2 v^4}{\alpha^2}}, \quad \mu = \frac{m_1 m_2}{m_1 + m_2} \quad (44)$$

and $H_{i\nu}^{(1)}(i\nu\epsilon)$ is the Hankel function of the first kind:

$$H_n^{(1)}(z) = J_n(z) + iY_n(z). \quad (45)$$

In Eq. (43), $(e_{em})_1$, m_1 and $(e_{em})_2$, m_2 are the electric charge and mass of the two colliding particles, while $\alpha = C^R \alpha_s$ is the strong coupling constant multiplied by the corresponding Casimir factor C^R for the channel under study:

$$C^8 = 4/3; \quad C^1 = 1/6; \quad C^6 = 2/3; \quad C^{\bar{3}} = 1/3.$$

When the interaction is repulsive (namely in the octet channel for the $q\bar{q}$ scattering, and in the sextet channel for the qq and $\bar{q}\bar{q}$ scatterings), Eq. (43) gets modified as follows:

$$\begin{aligned} \frac{d\mathcal{E}_\omega}{d\omega} &= \frac{2\pi\alpha^2\omega^2}{3v^4} \left(\frac{(e_{em})_1}{m_1} - \frac{(e_{em})_2}{m_2} \right)^2 \left\{ \left[H_{i\nu}^{(1)'}(i\nu\epsilon) \right]^2 \right. \\ &\quad \left. + \frac{\epsilon^2 - 1}{\epsilon^2} \left| H_{i\nu}^{(1)}(i\nu\epsilon) \right|^2 \right\} \exp[-2\pi\nu]. \end{aligned} \quad (46)$$

We consider quark matter with three equal mass light flavors, namely $m_1 = m_2 = m$; $\mu = m/2$. The total density of quarks and antiquarks can be obtained for example from the PNJL model (see Appendix B).

$$n_q \simeq 2.8T^3 \simeq 0.12 \text{ GeV}^3.$$

The total energy radiated in unit volume throughout the time of the collision in the case of Coulomb scattering can be obtained from the following formula:

$$\begin{aligned} \frac{d\Sigma}{d\omega} = & \frac{4\pi^2\alpha_{em}\omega^2}{3v^4} \frac{n_q^2}{18^2 m^2} \int_0^{b_{max}} \left[\left(\frac{4}{3}\alpha_s\right)^2 f\left(\frac{4}{3}\alpha_s\right) + 8 \left(\frac{1}{6}\alpha_s\right)^2 f\left(\frac{1}{6}\alpha_s\right) \exp[-2\pi\nu\alpha_s/6] \right. \\ & \left. + 3 \left(\frac{2}{3}\alpha_s\right)^2 f\left(\frac{2}{3}\alpha_s\right) + 6 \left(\frac{1}{3}\alpha_s\right)^2 f\left(\frac{1}{3}\alpha_s\right) \exp[-2\pi\nu\alpha_s/3] \right] b db, \end{aligned} \quad (47)$$

where

$$f(\alpha) = \left[H_{i\nu}^{(1)'}(i\nu\epsilon) \right]^2 + \frac{\epsilon^2 - 1}{\epsilon^2} \left| H_{i\nu}^{(1)}(i\nu\epsilon) \right|^2. \quad (48)$$

Eq. (47) is the total radiated energy, it takes into account all possible color channels for qq , $q\bar{q}$ and $\bar{q}\bar{q}$ scatterings, and all possible flavor combinations. b_{max} can be estimated directly from the quark density: in our temperature regime, it turns out that $b_{max} \simeq 1 \text{ GeV}^{-1}$. Our results for the ratio of the total energy radiated throughout the collision time in the case of quark-quark and quark-monopole scattering are shown in Figs. 6. The left panels show this ratio for $b_{max} \rightarrow \infty$, while in the right panels b_{max} is finite and fixed by the corresponding densities. This is useful to understand how strongly a finite b_{max} influences our results: it turns out that the cutoff dependence of $d\Sigma/d\omega$ is dramatic. Without cutoff, this quantity is much larger in the case of a Coulomb scattering, while the opposite is true in the case of a finite b_{max} . This effect is qualitatively true for all values of v that we have considered, but obviously the relative magnitude for qq and qM scatterings depends on the specific value of v that we choose.

4.2 Validity of our approximations

Our results are obtained through a series of approximations:

- non-relativistic approximation: this is obviously valid if the velocity v of quarks is not too large compared to the speed of light, namely $v \ll 1$;
- dipole approximation vs retarded emission. It is valid if the radiation wavelength is large. The retardation effects can be neglected in cases where the distribution of charge changes little during the time a/c , where a is the order of magnitude of the dimensions of the system. This is true if $v \ll 1$, which coincides with the condition for the non-relativistic approximation;
- classical trajectory is used, without back reaction of radiation: in all our formulas, we assume that the particle moves along a trajectory which is the solution of the classical equations of motion. This means that the energy lost by the particle through the radiation process is negligible. This approximation is valid in the limit $\omega \ll m/e^2$;

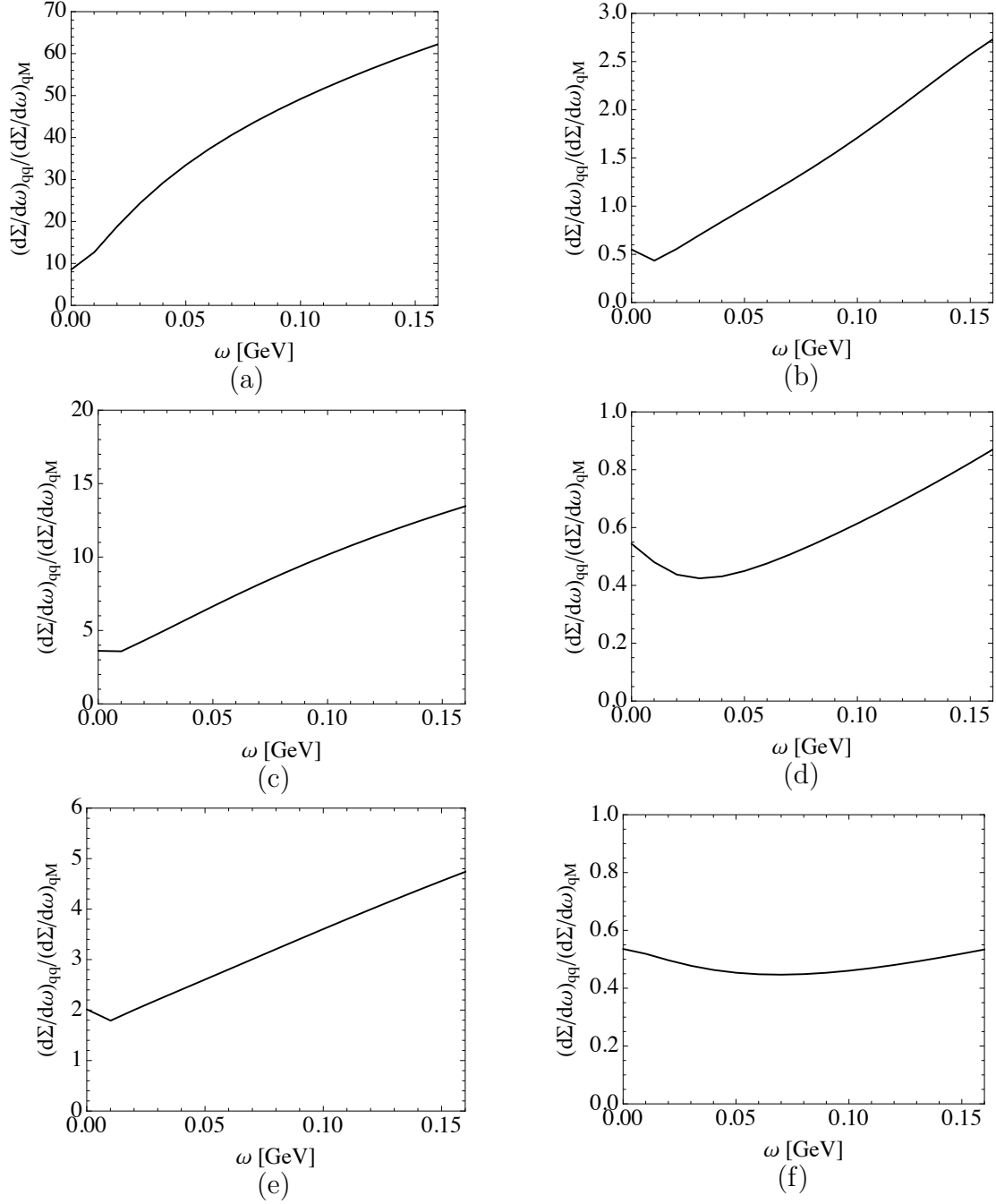


Figure 6: Left column: ratio of $d\Sigma/d\omega$ for Coulomb and quark-monopole scattering. In both cases, the integral over b is taken up to ∞ . For these plots we use $\alpha_s = 0.8$, $m = 0.3$ GeV and: (a) $v = 0.3$, (c) $v = 0.5$, (e) $v = 0.7$. Right column: same as in the left column, but the integral over b is taken up to the corresponding b_{max} . For these plots we use $\alpha_s = 0.8$, $m = 0.3$ GeV and: (b) $v = 0.3$, (d) $v = 0.5$, (f) $v = 0.7$.

- classical approximation: naively, the emission of soft photons can be described classically for

$$\hbar \omega \ll E_k = \mu v^2/2 = m v^2/4.$$

Within the same approximation we can ignore the recoil effect (energy-momentum conservation).

The full quantum treatment of the radiation should include the back reaction of the radiation, one has to evaluate the *nondiagonal* matrix element of the dipole moment between the initial and final scattering states, with different energies. Such quantum states for quark-monopole problem were found in [24] and recently for gluon-monopole problem in [13]. However, the matrix elements have not been computed yet. Since it was done for quantum Coulomb scattering, by A.Sommerfield in 1931, we can use those results in order to have at least some qualitative estimate for the accuracy of classical description.

We compare the total radiation $d\kappa_\omega$ in a given frequency interval $d\omega$, in the case of scattering on a single particle, namely we integrate over the impact parameter b from 0 to ∞ . In the classical case we have:

$$\frac{d\kappa_\omega}{d\omega} = \frac{32\pi^2\omega\alpha_{em}\alpha_s^3}{3m^3v^5} \left| H_{iv}^{(1)}(i\nu) \right| H_{iv}^{(1)'}(i\nu) \quad (49)$$

which is to be compared to the quantum expression [25]:

$$\frac{d\kappa(\omega)}{d\omega} = \alpha_{em}\alpha_s^2 \frac{64\pi^2}{3} \frac{p'}{p} \frac{1}{(p-p')^2} \frac{1}{(1-e^{-2\pi\beta'})(e^{2\pi\beta}-1)} \left(-\frac{d}{d\xi} |F(\xi)|^2 \right) \quad (50)$$

where

$$\beta = \frac{\alpha_s}{v} \quad \beta' = \frac{\alpha_s}{v'} \quad m v = 2 p \quad m v' = 2 p' \quad p' = \sqrt{p^2 - m \omega}$$

and

$$F(\xi) \equiv {}_2F_1(i\beta', i\beta; 1; \xi) \quad \xi = -\frac{4pp'}{(p-p')^2}$$

${}_2F_1(a, b; c; d)$ is the Hypergeometric function. The two curves corresponding to classical and quantum scatterings are shown in Fig. 7. It is thus evident that within the energy region plotted the classical result is a very good approximation of the quantum one. Note that there is a maximum ω , which is equal to the energy of the incoming particle beyond which due to energy conservation the quantum formula are not applicable.

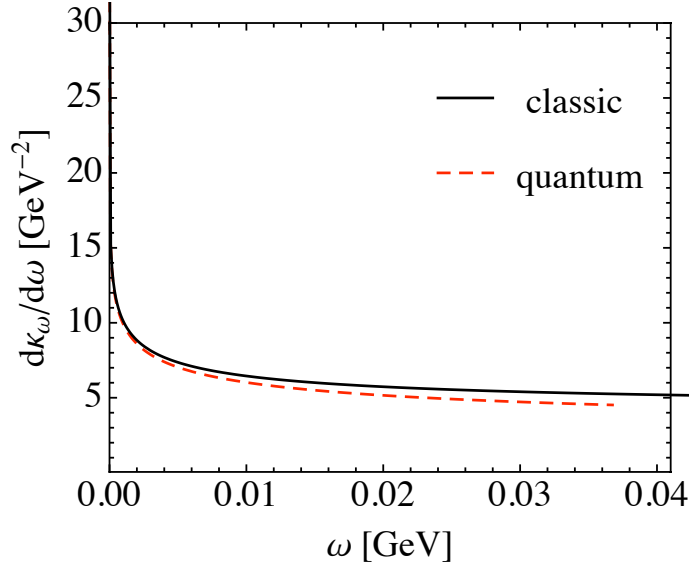


Figure 7: Comparison between classic and quantum result for $d\kappa_\omega/d\omega$ as a function of ω , with $\alpha_s = 0.8$, $v = 0.7$, $m = 0.3$ GeV.

- two body vs many body scattering. So far, we have limited our analysis to two-body scattering, while mimicking the effects of multiple interactions by finite quark and monopole densities and the maximal impact parameter. The strong dependence on the maximal impact parameter cutoff observed in our results, reflects additional shortcomings of our approach. The origin of this problem is obvious: on the one hand soft radiation is emitted from large distances; on the other hand, too large distances are precisely governed by multiple scattering.

5 Conclusions and outlook

The present paper is the first step towards understanding whether the contribution of the quark-monopole scattering process in QGP is or is not important for photon and dilepton production. Our purpose at present was pretty modest: we wanted to evaluate the magnitude of soft photon radiation from this process and compare it to the one produced in Coulomb quark-quark scattering. A qualitative estimate outlined in the Introduction, said that while the monopole density is small at high T , $n_m \sim (1/\ln(T))^3$, the square of α_s in the electric scattering cross section compensates two out of three such logarithms. So, parametrically, the process we consider is subleading at very large $\ln(T)$. On the other hand, the charge-monopole scattering at large angles and small impact parameter tends to be much larger than the charge-

charge one: we found that this enhances radiation, similarly to how it worked for transport processes [13]. This represents an encouraging starting point for future work.

We have calculated the photon radiation rate for quarks scattering on monopoles in a thermal medium which contains a finite density of both particles. We worked in the classic, non-relativistic approximation and neglected retardation effects and back reaction. Therefore, our calculation has a rather methodological status, it cannot address the actual phenomenological questions, such as the experimentally observed excess in dilepton production at small p_t and invariant mass below m_ρ . We need to improve the present paper in many directions: first of all, a full quantum and relativistic calculation will be performed, also taking into account back reaction of the radiation. This can in principle be done using non-diagonal matrix elements, calculated between quantum scattering states such as those which were found in [13, 24].

Then we need to take into account the fireball evolution, in order to be able to quantitatively compare our results to the experimental data. Dramatic expansion of the fireball and long duration of the near- T_c phase leads to the conclusion that soft dileptons currently constituting the puzzle come from the end of the evolution of QGP, $T \sim 1T_c$, rather than the beginning of it, in the temperature regime we discussed above. Unfortunately, the near- T_c region is very complicated and quite challenging theoretically. In this region monopoles become lighter and thus dynamical and relativistic, matter is no longer an electric near-perturbative plasma with at least well-defined counting rules, but a strongly coupled liquid made of all kind of quasiparticles. We hope to address those issues elsewhere in our future work.

Acknowledgments

This work is partially supported by the DOE grants DE-FG02-88ER40388 and DE-FG03-97ER4014 and by the DFG grant SFB-TR/55.

Appendix A

In this Appendix we explicitly calculate the Fourier transform of the \vec{a} components. We start from $(a_x)_\omega$:

$$(a_x)_\omega = -\frac{(eg)^2}{m^2 b^2 v \xi} \int_{-\infty}^{\infty} \frac{\exp[i\bar{\omega}t] \cos[\xi \arctan t]}{(t^2 + 1)^{3/2}} dt. \quad (51)$$

If we set $t = i + i\tau$, $dt = i d\tau$. Both the square root and the arctan have branch cut singularities from $\tau = 0$ to $\tau = \infty$ and from $\tau = -\infty$ to $\tau = -2$. This is clear if we

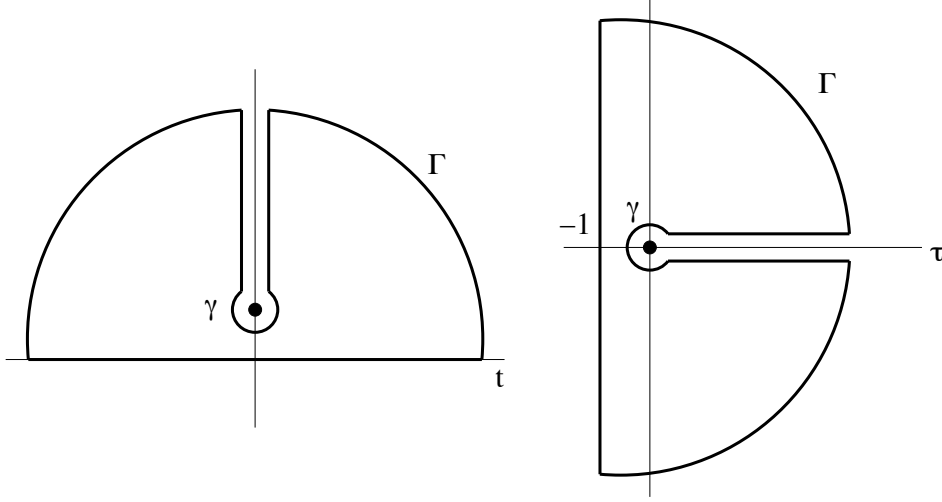


Figure 8: Integration contours in the complex t and τ planes.

write the relationship between arctan and log:

$$\arctan(i + i\tau) = i \operatorname{arctanh}(1 + \tau) = i \log \left(-\frac{2 + \tau}{\tau} \right). \quad (52)$$

We calculate the integral along the contour C shown in Fig. 8. The integral can be split into four different contributions:

- the small circle γ of radius ϵ
- the upper and lower segments around the branch cut
- the big circle Γ

We have

$$\begin{aligned} \int_{-\infty}^{\infty} \frac{\exp[i\bar{\omega}t] \cos[\xi \arctan t]}{(t^2 + 1)^{3/2}} dt &= \\ &= i \exp[-\bar{\omega}] \left\{ \int_{\epsilon}^{\infty} + \int_{\Gamma} + \int_{-\infty}^{\epsilon} + \int_{\gamma} \right\} \frac{\exp[-\bar{\omega}\tau] \cos[\xi \arctan(i + i\tau)]}{(-2\tau - \tau^2)^{3/2}} d\tau. \end{aligned} \quad (53)$$

Along the upper segment, where $\tau \rightarrow \tau + i\epsilon$, we have:

$$\begin{aligned} (-2\tau - \tau^2)^{3/2} &= -i (2\tau + \tau^2)^{3/2} \\ \log \left(-\frac{2 + \tau}{\tau} \right) &= \log \left| \frac{2 + \tau}{\tau} \right| + i\pi \end{aligned} \quad (54)$$

while along the lower one we have

$$\begin{aligned} (-2\tau - \tau^2)^{3/2} &= i(2\tau + \tau^2)^{3/2} \\ \log\left(-\frac{2+\tau}{\tau}\right) &= \log\left|\frac{2+\tau}{\tau}\right| - i\pi. \end{aligned} \quad (55)$$

Therefore we can write:

$$\begin{aligned} \left\{ \int_{\epsilon}^{\infty} + \int_{\infty}^{\epsilon} \right\} \frac{\exp[-\bar{\omega}\tau] \cos[\xi \arctan(i + i\tau)]}{(-2\tau - \tau^2)^{3/2}} d\tau &= \\ \int_{\epsilon}^{\infty} \frac{\exp[-\bar{\omega}\tau] \cos\left[\frac{i\xi}{2} \left(\log\left|\frac{2+\tau}{\tau}\right| + i\pi\right)\right]}{-i(2\tau + \tau^2)^{3/2}} d\tau + \int_{\infty}^{\epsilon} \frac{\exp[-\bar{\omega}\tau] \cos\left[\frac{i\xi}{2} \left(\log\left|\frac{2+\tau}{\tau}\right| - i\pi\right)\right]}{i(2\tau + \tau^2)^{3/2}} d\tau \\ &= 2i \cos\left(\frac{\xi\pi}{2}\right) \int_{\epsilon}^{\infty} \frac{\exp[-\bar{\omega}\tau] \cos\left[\frac{i\xi}{2} \log\left|\frac{2+\tau}{\tau}\right|\right]}{(2\tau + \tau^2)^{3/2}} d\tau \end{aligned} \quad (56)$$

where we used the relationship

$$\cos\alpha + \cos\beta = 2 \cos\frac{\alpha + \beta}{2} \cos\frac{\alpha - \beta}{2}. \quad (57)$$

We therefore have:

$$\begin{aligned} \left\{ \int_{\epsilon}^{\infty} + \int_{\infty}^{\epsilon} \right\} \frac{\exp[-\bar{\omega}\tau] \cos[\xi \arctan(i + i\tau)]}{(-2\tau - \tau^2)^{3/2}} d\tau &= \\ &= i \cos\left(\frac{\xi\pi}{2}\right) \int_{\epsilon}^{\infty} \frac{\exp[-\bar{\omega}\tau]}{(2\tau + \tau^2)^{3/2}} \left[\left(\frac{2+\tau}{\tau}\right)^{-\xi/2} + \left(\frac{2+\tau}{\tau}\right)^{\xi/2} \right] d\tau. \end{aligned} \quad (58)$$

The above integral contains two terms. The first one gives (in the limit $\epsilon \rightarrow 0$):

$$\begin{aligned} i \cos\left(\frac{\xi\pi}{2}\right) \int_0^{\infty} \frac{\exp[-\bar{\omega}\tau]}{(2\tau + \tau^2)^{3/2}} \left(\frac{2+\tau}{\tau}\right)^{-\xi/2} d\tau &= \\ &= i \cos\left(\frac{\xi\pi}{2}\right) \frac{1}{4} \Gamma\left[\frac{1}{2}(\xi - 1)\right] U\left(\frac{1}{2}(\xi - 1), -1, 2\bar{\omega}\right). \end{aligned} \quad (59)$$

The second term needs to be integrated by parts p times, where p is the smallest integer number $> \frac{\xi+3}{2}$. All boundary terms are either divergent or vanishing as $\epsilon \rightarrow 0$. The divergent ones are exactly cancelled by corresponding divergent terms

coming from the integral over the small circle γ . The finite part is:

$$\begin{aligned}
& \int_{\epsilon}^{\infty} \frac{\exp(-\bar{\omega}\tau) (2+\tau)^{(\xi-3)/2}}{\tau^{(\xi+3)/2}} d\tau = \frac{4\Gamma\left(\frac{\xi+3}{2} - p\right) p!}{\xi^2 - 1} \sum_{k=0}^p \frac{(-\bar{\omega})^k}{k!(p-k)!\Gamma\left(\frac{\xi-3}{2} - p + k + 1\right)} \times \\
& \times \int_0^{\infty} \exp(-\bar{\omega}\tau) [2+\tau]^{(\xi-3)/2-(p-k)} \tau^{p-(\xi+3)/2} d\tau = \\
& = \frac{4\Gamma\left(\frac{\xi+3}{2} - p\right) p!}{\xi^2 - 1} \sum_{k=0}^p \frac{(-\bar{\omega})^k}{k!(p-k)!\Gamma\left(\frac{\xi-3}{2} - p + k + 1\right)} \times \\
& \times 2^{k-2} \Gamma\left(p - \frac{\xi+1}{2}\right) U\left(p - \frac{\xi+1}{2}, k-1, 2\bar{\omega}\right).
\end{aligned} \tag{60}$$

The above contribution vanishes for odd, integer values of ξ . The contribution coming from Γ vanishes identically, while we get a nonvanishing contribution from the integral over the small circle γ . This contribution is divergent for noninteger or even ξ , exactly cancelling the divergent contribution coming from the segments along the branch cut. When ξ is an odd integer number we get a finite contribution. We redefine $t = i + i\epsilon \exp(i\theta)$, $dt = -\epsilon \exp(i\theta) d\theta$ and get:

$$\begin{aligned}
& \int_{\gamma} \frac{\exp[-\bar{\omega}\tau] \cos[\xi \arctan(i + i\tau)]}{(-2\tau - \tau^2)^{3/2}} d\tau \\
& = -\epsilon e^{-\bar{\omega}} \int_0^{2\pi} \frac{e^{i\theta} e^{-\epsilon \bar{\omega} e^{i\theta}} \cos[\xi \arctan(i + i\epsilon \exp(i\theta))]}{(-2\epsilon \exp(i\theta) - \epsilon^2 \exp(2i\theta))^{3/2}} d\theta \\
& = -\epsilon e^{-\bar{\omega}} \int_0^{2\pi} \frac{e^{i\theta} e^{-\epsilon \bar{\omega} e^{i\theta}}}{(-2\epsilon \exp(i\theta) - \epsilon^2 \exp(2i\theta))^{3/2}} \cos\left[\frac{\xi}{2i} \log\left(-\frac{\epsilon e^{i\theta}}{2 + \epsilon e^{i\theta}}\right)\right] d\theta \\
& = \frac{e^{-\bar{\omega}}}{2(-\epsilon)^{1/2}} \int_0^{2\pi} \frac{e^{-i\theta/2} e^{-\epsilon \bar{\omega} e^{i\theta}}}{(2 + \epsilon \exp(i\theta))^{3/2}} \left[\left(-\frac{\epsilon e^{i\theta}}{2 + \epsilon e^{i\theta}}\right)^{\xi/2} + \left(-\frac{\epsilon e^{i\theta}}{2 + \epsilon e^{i\theta}}\right)^{-\xi/2} \right] d\theta
\end{aligned} \tag{61}$$

For $\epsilon \rightarrow 0$, the first term in the parenthesis gives a finite contribution only for $\xi = 1$, a value which is never reached in practical cases, as we will see. For $\xi > 1$ its

contribution vanishes identically. The second term gives

$$\begin{aligned}
& \frac{e^{-\bar{\omega}}}{2(-\epsilon)^{1/2}} \int_0^{2\pi} \frac{e^{-i\theta/2} e^{-\epsilon\bar{\omega}e^{i\theta}}}{(2 + \epsilon e^{i\theta})^{3/2}} \left(-\frac{\epsilon e^{i\theta}}{2 + \epsilon e^{i\theta}} \right)^{-\xi/2} d\theta = \\
& = \frac{e^{-\bar{\omega}}}{2} \int_0^{2\pi} \frac{e^{-2i\theta} e^{-\epsilon\bar{\omega}e^{i\theta}} (2e^{-i\theta} + \epsilon)^{(\xi-3)/2}}{(-\epsilon)^{(\xi+1)/2}} d\theta = \\
& = \frac{e^{-\bar{\omega}}}{2(-\epsilon)^{(\xi+1)/2}} \int_0^{2\pi} d\theta e^{-2i\theta} \sum_{n=0}^{\infty} \frac{\omega^n (-\epsilon)^n e^{in\theta}}{n!} \sum_{k=0}^{(\xi-3)/2} \frac{(2e^{-i\theta})^k \epsilon^{(\xi-3)/2-k} (\frac{\xi-3}{2})!}{k! (\frac{\xi-3}{2} - k)!} = \\
& = \frac{e^{-\bar{\omega}}}{2} \int_0^{2\pi} d\theta e^{-2i\theta} \sum_{k=0}^{(\xi-3)/2} \frac{\omega^{k+2}}{(k+2)!} \frac{(-1)^{k-(\xi-3)/2} 2^k e^{2i\theta} (\frac{\xi-3}{2})!}{k! (\frac{\xi-3}{2} - k)!} = \\
& = \frac{e^{-\bar{\omega}}}{2} 2\pi \sum_{k=0}^{(\xi-3)/2} \frac{\omega^{k+2}}{(k+2)!} \frac{(-1)^{k-(\xi-3)/2} 2^k (\frac{\xi-3}{2})!}{k! (\frac{\xi-3}{2} - k)!} \tag{62}
\end{aligned}$$

where we have taken into account the fact that the finite contribution from the sum over n comes from $n = k + 2$. The final result for $(a_x)_\omega$ is therefore

$$\begin{aligned}
(a_x)_\omega &= \frac{(eg)^2}{m^2 b^2 v \xi} \left\{ \exp(-\bar{\omega}) \cos\left(\frac{\pi\xi}{2}\right) \left[\frac{1}{4} \Gamma\left(\frac{1}{2}(\xi-1)\right) U\left(\frac{1}{2}(\xi-1), -1, 2\bar{\omega}\right) \right. \right. \\
&+ \frac{4p! \Gamma(-p + \frac{\xi+3}{2})}{\xi^2 - 1} \sum_{k=0}^p \frac{(-\bar{\omega})^k}{k! (p-k)! \Gamma(\frac{\xi-3}{2} - p + k + 1)} \times \tag{63}
\end{aligned}$$

$$\left. \left. \times 2^{k-2} \Gamma\left(p - \frac{\xi+1}{2}\right) U\left(p - \frac{\xi+1}{2}, k-1, 2\bar{\omega}\right) \right] \right\} \tag{64}$$

for any value of ξ other than odd-integer, and

$$(a_x)_\omega = \frac{(eg)^2}{m^2 b^2 v \xi} \frac{e^{-\bar{\omega}}}{2} 2\pi \sum_{k=0}^{(\xi-3)/2} \frac{\omega^{k+2}}{(k+2)!} \frac{(-1)^{k-(\xi-3)/2} 2^k (\frac{\xi-3}{2})!}{k! (\frac{\xi-3}{2} - k)!}. \tag{65}$$

for odd-integer ξ .

The component $(a_y)_\omega$ slightly differs from $(a_x)_\omega$: the sin integration gives a purely imaginary contribution. The second term in Eq. (63) has a minus sign.

The first terms of the components expansion around $\omega = 0$ have the following asymptotic behavior:

$$\begin{aligned}
(a_x)_{\omega \rightarrow 0} \simeq & \frac{2v}{\xi} \cos \left[\frac{\pi\xi}{2} \right] + \omega^2 \frac{b^2(\xi^2 - 1)}{v\xi} \cos \left[\frac{\pi\xi}{2} \right] \left\{ -\frac{1}{\xi^2 - 1} \right. \\
& + \frac{1}{2} \left[-\text{Harmonicnumber} \left(p - \frac{\xi + 3}{2} \right) - \text{Harmonicnumber} \left(\frac{\xi + 1}{2} \right) \right. \\
& + \frac{1}{\xi^2 - 1} (-3 - 2p^2 - 2p(\xi - 2) - 2\gamma(\xi^2 - 1) + \xi(4 - \xi(-3 + \ln 4)) \\
& + \ln 4 - 2(\xi^2 - 1) \ln \frac{b}{v} \omega) \left. \right] + \theta(p - 3) \frac{4p! \Gamma \left[-p + \frac{\xi + 3}{2} \right]}{\xi^2 - 1} \sum_{k=3}^p \frac{(-1)^k (k - 3)!}{k! (p - k)! \Gamma \left[\frac{\xi - 3}{2} - p + k + 1 \right]} \left. \right\}
\end{aligned} \tag{66}$$

$$(a_y)_{\omega \rightarrow 0} \simeq 2ib \cos \left[\frac{\pi\xi}{2} \right] \omega$$

$$(a_z)_{\omega \rightarrow 0} \simeq -\frac{(eg)v}{\sqrt{(eg)^2 + (m vb)^2}} - \omega^2 \left[\frac{b^2 eg (-1 + 2\gamma + 2 \ln \omega + 2 \ln (\frac{b}{2v}))}{2v \sqrt{(eg)^2 + (m vb)^2}} \right]$$

where $\text{Harmonicnumber}(z) = \Psi(z + 1) + \gamma$ and γ is the Euler's constant and $\Psi(z)$ is the logarithmic derivative of Γ -function.

Appendix B

In this appendix we briefly recall some aspects of the PNJL model [26], which we will then use to calculate the density of quarks in the medium. This model successfully describes QCD thermodynamics in the temperature regime we are interested in, by coupling quarks to the chiral condensate and to a temporal background gauge field related to the Polyakov loop. The Euclidean action of the three-flavor PNJL model is

$$\mathcal{S}_E(\psi, \psi^\dagger, \phi) = \int_0^{\beta=1/T} d\tau \int_V d^3x [\psi^\dagger \partial_\tau \psi + \mathcal{H}(\psi, \psi^\dagger, \phi)] - \frac{V}{T} \mathcal{U}(\phi, T). \tag{67}$$

Here \mathcal{H} is the fermionic Hamiltonian density given by:

$$\mathcal{H} = -i\psi^\dagger (\vec{\alpha} \cdot \vec{\nabla} + \gamma_4 m_0 - \phi) \psi + \mathcal{V}(\psi, \psi^\dagger), \tag{68}$$

where ψ is the $N_f = 3$ quark field, $\vec{\alpha} = \gamma_0 \vec{\gamma}$ and $\gamma_4 = i\gamma_0$ in terms of the standard Dirac γ matrices and $m_0 = \text{diag}(m_{0u}, m_{0d}, m_{0s})$ is the current quark mass matrix.

$\mathcal{V}(\psi, \psi^\dagger)$ contains two parts: a four-fermion interaction acting in the pseudoscalar-isovector/scalar-isoscalar quark-antiquark channel, and a six-fermion interaction which breaks $U_A(1)$ symmetry explicitly:

$$\begin{aligned} \mathcal{V}(\psi, \psi^\dagger) = & - \frac{G}{2} \sum_{f=u,d,s} \left[(\bar{\psi}_f \psi_f)^2 + (\bar{\psi}_f i\gamma_5 \vec{\tau} \psi_f)^2 \right] \\ & + \frac{K}{2} \left[\det_{i,j} (\bar{\psi}_i (1 + \gamma_5) \psi_j) + \det_{i,j} (\bar{\psi}_i (1 - \gamma_5) \psi_j) \right] \end{aligned} \quad (69)$$

Quarks move in a background color gauge field $\phi \equiv A_4 = iA_0$, where $A_0 = \delta_{\mu 0} g \mathcal{A}_a^\mu t^a$ with the $SU(3)_c$ gauge fields \mathcal{A}_a^μ and the generators $t^a = \lambda^a/2$. The matrix valued, constant field ϕ relates to the (traced) Polyakov loop as follows:

$$\Phi = \frac{1}{N_c} \text{Tr} \left[\mathcal{P} \exp \left(i \int_0^\beta d\tau A_4 \right) \right] = \frac{1}{3} \text{Tr} e^{i\phi/T}. \quad (70)$$

The thermodynamic potential of the system is:

$$\begin{aligned} \Omega(T, \mu) = & \mathcal{U}(\Phi, T) + \frac{\sigma_{u,d}^2}{2G} + \frac{\sigma_s^2}{4G} - \frac{K}{4G^3} \sigma_{u,d}^2 \sigma_s \\ & - 2 \sum_f T \int \frac{d^3 p}{(2\pi)^3} \left\{ \ln \left[1 + \Phi e^{-(E_{p,f} - \mu_f)/T} + \Phi e^{-2(E_{p,f} - \mu_f)/T} + e^{-3(E_{p,f} - \mu_f)/T} \right] \right. \\ & \left. + \ln \left[1 + \Phi e^{-(E_{p,f} - \bar{\mu}_f)/T} + \Phi e^{-2(E_{p,f} - \bar{\mu}_f)/T} + e^{-3(E_{p,f} - \bar{\mu}_f)/T} \right] + 3 \frac{E_{p,f}}{T} \theta(\Lambda^2 - \vec{p}^2) \right\}. \end{aligned} \quad (71)$$

where

$$\sigma_i = 2G \langle \bar{\psi}_i \psi_i \rangle, \quad \bar{\mu}_f = -\mu_f, \quad E_{p,f} = \sqrt{\vec{p}^2 + m_f^2}, \quad m_i = m_{0i} - \sigma_i - \frac{K}{4G^2} \sigma_j \sigma_k. \quad (72)$$

By minimizing the thermodynamic potential one can obtain the behavior of the chiral condensates σ_i and of the Polyakov loop Φ as functions of the temperature and chemical potential. After this procedure, one is able to evaluate many thermodynamic quantities. For example, the quark density we are interested in is the sum of the densities of quarks and antiquarks and can be obtained through the following formula:

$$n_q = \frac{\partial \Omega}{\partial \mu_f} + \frac{\partial \Omega}{\partial \bar{\mu}_f} \quad (73)$$

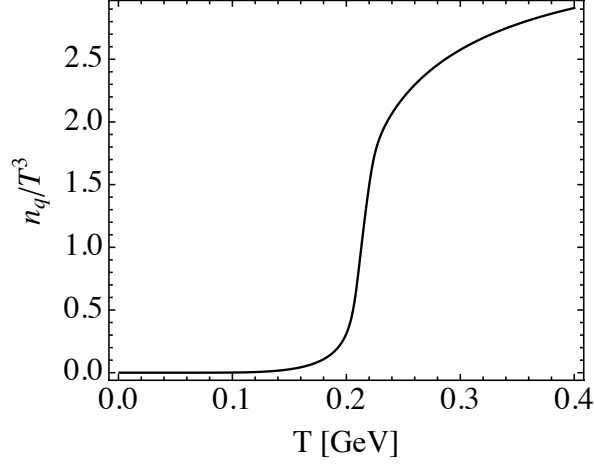


Figure 9: Total quark density as a function of the temperature (PNJL model result).

and it has the following explicit form:

$$n_q = \frac{N_f}{\pi^2 T^3} \int \left[\frac{3 \exp[\mu/T] (\exp[2\mu/T] + \Phi \exp[2E_p/T] + 2\Phi \exp[(E_p + \mu)/T])}{\exp[3E_p/T] + \exp[3\mu/T] + 3\Phi \exp[(2E_p + \mu)/T] + 3\Phi \exp[(E_p + 2\mu)/T]} \right. \\ \left. + \frac{3 (1 + \Phi \exp[2(E_p + \mu)/T] + 2\Phi \exp[(E_p + \mu)/T])}{1 + \exp[3(E_p + \mu)/T] + 3\Phi \exp[2(E_p + \mu)/T] + 3\Phi \exp[(E_p + \mu)/T]} \right] p^2 dp \quad (74)$$

We show the behavior of quark density in Fig. 9, for typical PNJL model parameters taken from the last paper of Ref. [26].

References

- [1] E. V. Shuryak, Phys. Lett. B **78**, 150 (1978) [Sov. J. Nucl. Phys. **28**, 408.1978 YAFIA,28,796 (1978 YAFIA,28,796-808.1978)].
- [2] G. Agakichiev *et al.* [CERES Collaboration], Eur. Phys. J. C **41**, 475 (2005) [arXiv:nucl-ex/0506002].
- [3] G. Usai *et al.* [NA60 Collaboration], Eur. Phys. J. C **43**, 415 (2005).
- [4] S. Afanasiev *et al.* [PHENIX Collaboration], arXiv:0706.3034 [nucl-ex];
A. Adare *et al.* [PHENIX Collaboration], arXiv:0804.4168 [nucl-ex].
- [5] K. Dusling and I. Zahed, Nucl. Phys. A **825**, 212 (2009) [arXiv:0712.1982 [nucl-th]].
K. Dusling, arXiv:0901.2027 [nucl-th].

- [6] S. Turbide, C. Gale, E. Frodermann and U. Heinz, Phys. Rev. C **77**, 024909 (2008) [arXiv:0712.0732 [hep-ph]].
- [7] R. Rapp, J. Wambach and H. van Hees, arXiv:0901.3289 [hep-ph].
H. van Hees and R. Rapp, Nucl. Phys. A **827**, 341C (2009) [arXiv:0901.2316 [nucl-th]].
- [8] K. O. Lapidus and V. M. Emelyanov, Phys. Part. Nucl. **40**, 29 (2009).
- [9] R. Arnaldi *et al.* [NA60 Collaboration], Eur. Phys. J. C **59**, 607 (2009) [arXiv:0810.3204 [nucl-ex]].
- [10] R. Rapp and E. V. Shuryak, Phys. Lett. B **473**, 13 (2000) [arXiv:hep-ph/9909348].
- [11] J. Liao and E. Shuryak, Phys. Rev. C **75**, 054907 (2007) [arXiv:hep-ph/0611131].
- [12] M. N. Chernodub and V. I. Zakharov, Phys. Rev. Lett. **98**, 082002 (2007) [arXiv:hep-ph/0611228].
- [13] C. Ratti and E. Shuryak, Phys. Rev. D **80**, 034004 (2009) [arXiv:0811.4174 [hep-ph]]. C. Ratti, arXiv:0907.4353 [hep-ph].
- [14] T. A. De Grand, D. Toussaint, Phys. Rev. D **22**, 2478 (1980).
- [15] A. D'Alessandro and M. D'Elia, Nucl. Phys. B **799**, 241 (2008) [arXiv:0711.1266 [hep-lat]].
- [16] P. Aurenche, F. Gelis, R. Kobes and H. Zaraket, Phys. Rev. D **58**, 085003 (1998) [arXiv:hep-ph/9804224]; F. Gelis, Nucl. Phys. A **698**, 436 (2002) [arXiv:hep-ph/0104067]; P. Aurenche, F. Gelis, G. D. Moore and H. Zaraket, JHEP **0212**, 006 (2002) [arXiv:hep-ph/0211036].
- [17] L. D. Landau, E. M. Lifshitz “TEXTBOOK ON THEORETICAL PHYSICS. VOL. 2: CLASSICAL FIELD THEORY.
- [18] Y. M. Shnir, *Berlin, Germany: Springer (2005) 532 p*
- [19] K. A. Milton, Rept. Prog. Phys. **69**, 1637 (2006) [arXiv:hep-ex/0602040].
- [20] D. G. Boulware, L. S. Brown, R. N. Cahn, S. D. Ellis and C. k. Lee, Phys. Rev. D **14**, 2708 (1976).
- [21] F. Karsch and M. Kitazawa, Phys. Lett. B **658**, 45 (2007) [arXiv:0708.0299 [hep-lat]].

- [22] F. Karsch and M. Kitazawa, arXiv:0906.3941 [hep-lat].
- [23] E. M. Ilgenfritz, K. Koller, Y. Koma, G. Schierholz, T. Streuer, V. Weinberg and M. Quandt, PoS **LAT2007**, 311 (2007) [arXiv:0710.2607 [hep-lat]].
- [24] Y. Kazama, C. N. Yang and A. S. Goldhaber, Phys. Rev. D **15**, 2287 (1977).
- [25] B Berestetskii, L. P. Pitaevskii, and E.M. Lifshitz, “TEXTBOOK ON THEORETICAL PHYSICS. VOL. 4: Quantum Electrodynamics”
- [26] P. N. Meisinger, T. R. Miller, and M. C. Ogilvie, Phys. Rev. D **65**, 034009 (2002); P. N. Meisinger, M. C. Ogilvie and T. R. Miller, Phys. Lett. B **585**, 149 (2004); K. Fukushima, Phys. Lett. B **591**, 277 (2004); C. Ratti, M. A. Thaler and W. Weise, Phys. Rev. **D73**, 014019 (2006); S. Roessner, C. Ratti and W. Weise, Phys. Rev. **D75**, 034007 (2007).